

PROCEEDINGS OF SPIE

[SPIDigitalLibrary.org/conference-proceedings-of-spie](https://spiedigitallibrary.org/conference-proceedings-of-spie)

The development and analysis of cryogenic optical systems for the rapid infrared imager/spectrometer

John Capone, David Content, Ori Fox, Neil Gehrels, Alexander Kuttyrev, et al.

John I. Capone, David A. Content, Ori D. Fox, Neil A. Gehrels, Alexander S. Kuttyrev, Gennadiy N. Lotkin, Samuel H. Moseley, Frederick D. Robinson, Vicki L. Toy, Sylvain Veilleux, Stuart N. Vogel, "The development and analysis of cryogenic optical systems for the rapid infrared imager/spectrometer," Proc. SPIE 8863, Cryogenic Optical Systems and Instruments 2013, 88630D (27 September 2013); doi: 10.1117/12.2023123

SPIE.

Event: SPIE Optical Engineering + Applications, 2013, San Diego, California, United States

The development and analysis of cryogenic optical systems for the rapid infrared imager/spectrometer

John I. Capone^{*a}, David A. Content^b, Ori D. Fox^{bc}, Neil A. Gehrels^b, Alexander S. Kutyrav^{ab},
Gennadiy N. Lotkin^{bd}, Samuel H. Moseley^b, Frederick D. Robinson^{bd}, Vicki L. Toy^a,
Sylvain Veilleux^a, Stuart N. Vogel^a

^aDept. of Astronomy, Univ. of Maryland/College Park, CSS Bldg., Rm. 1204, Stadium Dr., College Park, MD, USA 20742;

^bNASA's Goddard Space Flight Center, 8800 Greenbelt Rd., Greenbelt, MD, USA 20771;

^cDept. of Astronomy, Univ. of California/Berkeley, B-20 Hearst Field Annex #3411, Berkeley, CA, USA 94720;

^dGlobal Science & Technology, Inc., 7855 Walker Drive, Suite 200, Greenbelt, MD, USA 20770

ABSTRACT

The Observational Cosmology Laboratory at NASA's Goddard Space Flight Center (GSFC), in collaboration with the University of Maryland, is building the Rapid Infrared Imager/Spectrometer (RIMAS) for the new 4.3 meter Discovery Channel Telescope (DCT). The instrument is designed to observe gamma-ray burst (GRB) afterglows following their initial detection by the Swift satellite. RIMAS will operate in the near infrared (0.9 – 2.4 microns) with all of its optics cooled to ~60 K. The primary optical design includes a collimator lens assembly, a dichroic dividing the wavelength coverage into the "YJ band" and "HK band" optical arms, and camera lens assemblies for each arm. Additionally, filters and dispersive elements are attached to wheels positioned prior to each arm's camera, allowing the instrument to quickly change from its imaging modes to spectroscopic modes. Optics have also been designed to image the sky surrounding spectroscopic slits to help observers pass light from target sources through these slits. Because the optical systems are entirely cryogenic, it was necessary to account for changing refractive indices and model the effects of thermal contraction. One result of this work is a lens mount design that keeps lenses centered on the optical axis as the system is cooled. Efforts to design, tolerance and assemble these cryogenic optical systems are presented.

Keywords: cryogenic systems, astronomical instrumentation, optical design, near infrared, optomechanics, infrared spectroscopy

1. INTRODUCTION

The Discovery Channel Telescope (DCT) is a 4.3 meter optical telescope recently built by Lowell Observatory and Discovery Communications. The telescope is located near Happy Jack, Arizona at an elevation of 7,800 feet above sea level. After reflection off the primary and secondary mirrors, light is passed into an "instrument cube" located behind the primary mirror^{7,11}. The telescope operator may insert fold-mirrors to pass light into one of four instruments located on four of the cube's sides, or allow the light to continue un-reflected into the Large Monolithic Imager (LMI) at the bottom of the cube. Among the instruments scheduled for installation on the instrument cube during the first year of the DCT's operations is the **Rapid Infrared Imager/Spectrometer (RIMAS)**. The instrument is being built by a collaboration between the Observational Cosmology Laboratory at NASA's Goddard Space Flight Center (GSFC) and the University of Maryland, College Park (UMCP). RIMAS is designed to observe gamma-ray burst (GRB) afterglows as part of the Swift space observatory's science goals. Following the detection of a GRB, the DCT will slew to the burst's location when possible. RIMAS will then acquire photometric and spectroscopic data at near infrared (NIR) wavelengths of the afterglow emission. This new instrumentation is intended to compliment and improve on the efforts of the Reionization and Transients Infrared/Optical (RATIR) project, another recent GRB instrument built by the Observational Cosmology Laboratory. RATIR has been successfully acquiring scientific data since it's first light in the fall of 2012².

* jicapone@astro.umd.edu; phone 1 301 405-1557; fax 1 301 314-9067; lowell.edu/dct_instruments_rimas.php

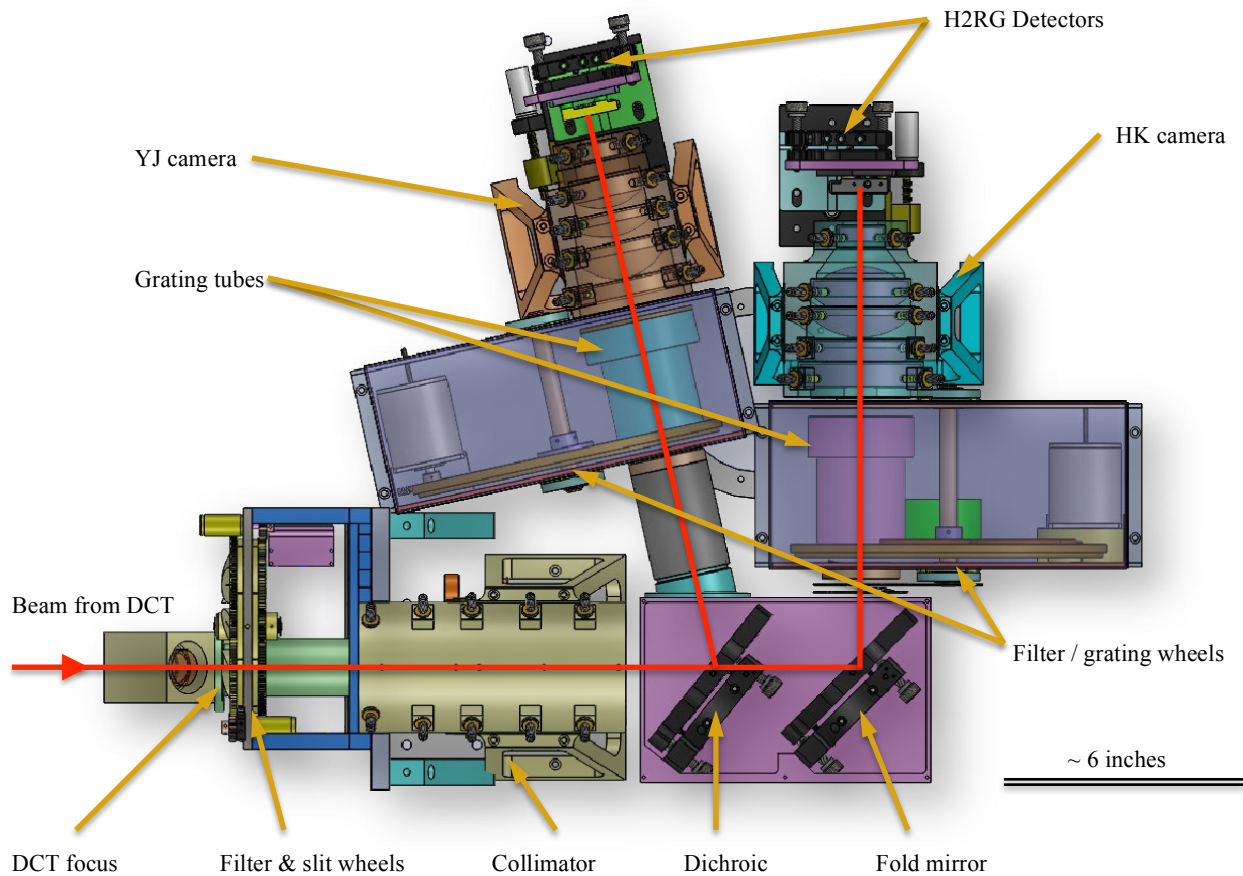


Figure 1. The drawing shows the layout of the optical and mechanical elements used in the RIMAS design. Light from the DCT first passes through the filter and slit wheels in the instrument’s “front module,” is collimated and continues until focused by either the “YJ-band” (0.9 – 1.4 μm) or “HK-band” (1.4 – 2.4 μm) camera.

2. RIMAS OPTICAL DESIGN

GRBs are the most energetic transient events in the Universe. Following the initial burst, which typically lasts a few seconds, an afterglow is emitted which is often observable across the electromagnetic spectrum. While afterglows may be detected for days or longer, the intensity of the emission drops off as a power-law with time. For this reason observatories must respond quickly to acquire the best possible data. Additionally, the pursuit of various scientific goals related to afterglows requires acquisition of photometric as well as low ($R \sim 25$) and moderate ($R \sim 4000$) spectral resolving power spectroscopic data³. RIMAS has been designed to address these needs by quickly changing between various acquisition configurations. Because the instrument will operate at NIR wavelengths (0.9 – 2.4 μm), the entire system will be cooled to cryogenic temperatures (~ 60 K) to reduce background from thermal emission, particularly at longer wavelengths.

2.1 Design Overview

RIMAS has been designed to operate as a camera and spectrograph at NIR wavelengths where the atmosphere is transparent. The fold mirror on the previously mentioned instrument cube allows a maximum field of view (FOV) of about 3 arcmin diameter. Before entering the main dewar, the beam enters a front module, an attachment to the dewar operating at ~ 60 K under vacuum. The attachment contains field-limiting slits, which can be placed at the focus of the telescope for use with the instrument’s spectroscopic modes. Slits of various sizes can be selected by rotating a wheel on which they are mounted. Although the final widths remain to be decided, it is likely that widths of 0.6 arcsec, 1 arcsec and 2 arcsec will be included. The surface surrounding each slit is tilted and covered in a flat mirror in order to reflect fields surrounding the slit into “slit-imaging” optics. These optics will image fields surrounding the slits on a small

(256×256 pixels) legacy indium antimonide (InSb) Spitzer IRCAM detector to help observers center light from their sources onto the slits. This detector's FOV will be approximately 80 arcsec diameter. The slit-wheel will also have an open slot for imaging modes and a pick-off mirror for the future installation of MOHSIS, a fiber-Bragg grating (FBG) atmospheric hydroxyl (OH) emission line suppressor^{12,13}. Near the slit-wheel, there is a second wheel which has eight positions for program-specific specialty filters. These filters are contained in the front dewar attachment so they may be replaced easily without disassembling the main dewar.

All of RIMAS's optics are kept cold ($T \sim 60$ K) within the instrument's double-dome dewar as well as within the front dewar attachment. These cooled optics reduce thermal background, which is most important at the long end of the instrument's wavelengths nearer $2.4 \mu\text{m}$. As light enters the dewar after passing through the front dewar attachment, the beam is collimated by a lens assembly before being separated by a dichroic into two optical arms. The first arm is for the Y and J bands ($0.97 - 1.07 \mu\text{m}$ and $1.17 - 1.33 \mu\text{m}$) and the second is for the H and K bands ($1.49 - 1.78 \mu\text{m}$ and $2.03 - 2.37 \mu\text{m}$). Near the pupil of each arm is a wheel which holds broad-band photometric filters as well as low ($R \sim 25$) and moderate ($R \sim 4,000$) spectral resolving power diffractive elements. Rotating these wheels allows the observer to select the operational mode of the instrument. After passing through either a filter or diffractive element, the light of each arm will be focused by camera optics onto a Teledyne HAWAII-2RG (H2RG) detector.

All of the wheels used in the design will be rotated by stepper motors, allowing the setup to be changed in less than ~ 15 seconds. Additionally, the optical bench will be cooled using a two-stage Sumitomo CH-208R cryocooler. The first stage will provide temperatures of ~ 60 K for the H2RG detectors and optics. The second stage will provide temperatures of ~ 15 K for the InSb detector.

2.2 Scientific optics

A drawing of RIMAS's optical and mechanical layout is shown in Figure 1. Some important design specifications of the main optical system are as follows:

- 3 arcmin imaging FOV
- 50% encircled energy from a point source within 0.35 arcsec as-built
- Plate scale of 0.35 arcsec per pixel (H2RG pixel pitch = $18 \mu\text{m}$)
- $F/\# = 2.53$
- Low resolution spectroscopy, $R \sim 25$
- Moderate resolution spectroscopy, $R \sim 4,000$

A lens system was selected rather than mirrors primarily because of the volume and weight requirements of the telescope. The design includes a total of 15 lenses, with 5 lenses per collimator or camera. Lens diameters range between 26.8 mm and 80.6 mm while center thicknesses range from 5 mm to 48.1 mm. Approximately half of the lenses have non-zero conic constant, and one lens includes a surface with a radial polynomial term. Lenses are fabricated from Infrasil, CaF_2 , ZnSe, S-TIH53, and BaF_2 .

The spectral coverage is divided into two bands, each with a filter/grating wheel, camera and detector. This was done primarily to improve the optical performance by allowing each optical arm to be designed for a narrower range of wavelengths. Additionally, using two detectors allows for the simultaneous acquisition of images in two photometric bands so that more data can be collected on GRB afterglows in a shorter amount of time.

Moderate resolution spectroscopy will be achieved for each optical arm by using multiple, cross-dispersed orders of blazed grating prisms (grisms). Simulated spectra are presented in Figure 2. The grisms will be produced at Lawrence Livermore National Laboratory (LLNL) where similar optics have been ruled for instruments including JWST's NIRISS^{4,5}. The group at LLNL has achieved RMS figure errors of ~ 0.02 wave⁶.

Tolerances were determined for the fabrication of optical elements and their optomechanical alignment by building a tolerancing function within Zemax ray-tracing software. This function was then used to perform a sensitivity analysis where individual parameters were changed to their minimum and maximum perturbed values to determine their relative impacts on the final system. Monte Carlo simulations were run to determine that the predicted final system performance was in compliance with the design specifications at the 90% probability level. Additionally, a tolerancing analysis done by Optical Support, Inc. during an independent review found similar tolerances. Average tolerances for important parameters are provided in Table 1. Discussions with lens manufacturers suggested that relevant tolerances were reasonable. Approximately half of these lenses have been delivered, with the remaining lenses expected by the end of the third quarter, 2013.

The alignment tolerances in Table 1 are challenging. It is planned to achieve these levels through a combination of precision machining of the lens mounting tubes and hand alignment aided by an alignment telescope equipped with a CostalOpt "pip-generator."

Table 1. Summarized results of the tolerancing analysis. Values are averaged over all lenses in the main optical system.

Parameter	Mean Tolerance
Substrate refractive index	$\pm 9e-4$
Surface radius of curvature	± 3.0 parts per thousand
Lens center thickness	$\pm 73 \mu\text{m}$
Lens wedge	$\pm 27 \mu\text{m}$
RMS surface irregularities	3.8 fringes
Axial position of lens (within mounting tubes)	$\pm 24.2 \mu\text{m}$
Tip/tilt of lens	± 1.1 arcmin
Decenter of lens from optical axis	$\pm 25 \mu\text{m}$

2.3 Spectroscopic slit-imaging optics

To aid observers in using the slitted, spectroscopic modes of the instrument, it was decided that the light blocked by the slits should be imaged on a Spitzer IRCAM legacy InSb detector. The system was designed to be as simple as possible since it is not intended for the acquisition of scientific data.

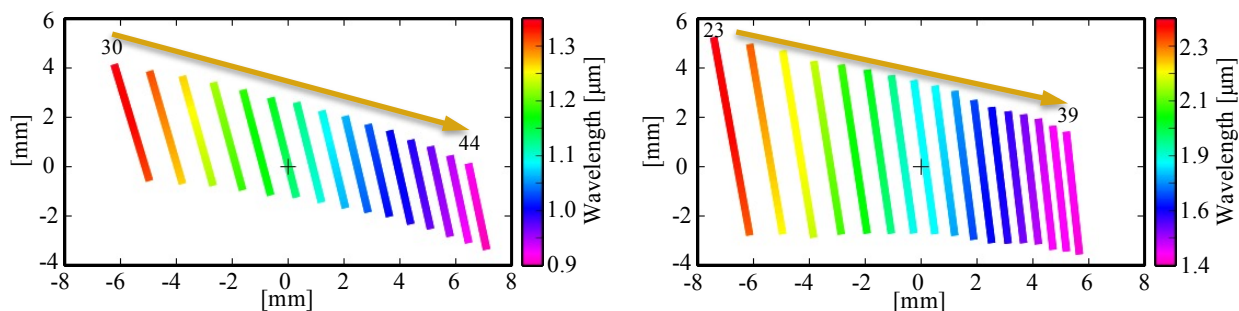


Figure 2. On the left is the modeled spectrum produced by the cross-dispersed YJ-band grism. The right plot shows the same for the HK-band grism. The numbers and arrows above the spectra represent the grism diffraction orders.

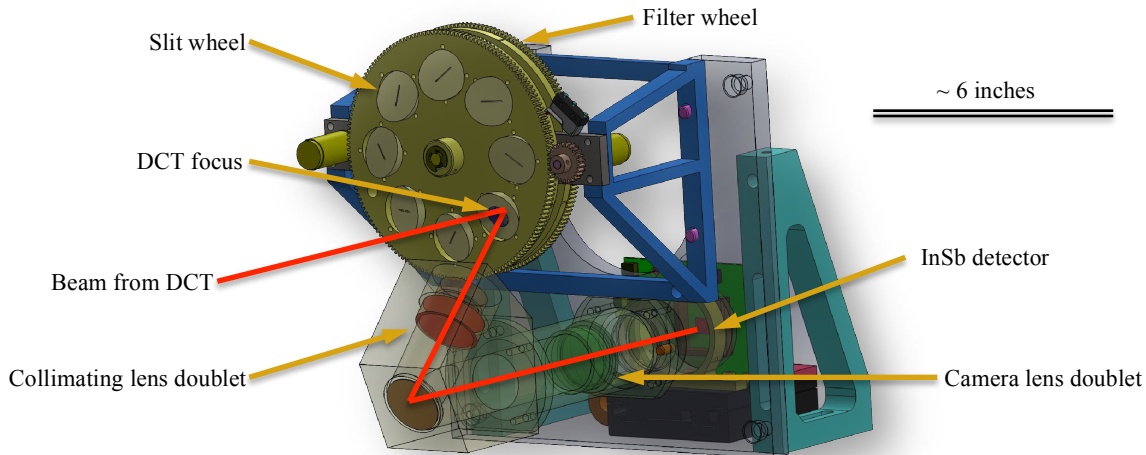


Figure 3. Drawing of the slit-imaging camera. Light from the DCT is reflected off a mirrored surface surrounding spectroscopic slits and passed into the imaging system as shown.

The design specifications are as follows:

- 80 arcsec FOV
- Plate scale of 0.35 arcsec per pixel (InSb pixel pitch = 30 μm)
- $F/\# = 4.21$

Table 2. Summarized results of tolerancing analysis. Values are averaged over all slit-imaging lenses.

Parameter	Mean Tolerance
Substrate refractive index	$\pm 1\text{e-}3$
Surface radius of curvature	± 23 parts per thousand
Lens center thickness	$\pm 225 \mu\text{m}$
Lens wedge	$\pm 88 \mu\text{m}$
RMS surface irregularities	2.5 fringes
Axial position of lens	$\pm 190 \mu\text{m}$
Tip/tilt of lens	± 6 arcmin
Decenter of lens from optical axis	$\pm 190 \mu\text{m}$

The design, shown in Figure 3, is relatively simple, requiring only four lenses to meet the optical specifications while conforming to the mechanical constraints. Relatively loose tolerances were determined using an analysis similar to that performed for the main optical system (see Table 2). All four lenses in this design have been delivered and are AR coated.

3. THERMAL EFFECTS

Because the primary optics were designed for the operating temperature of $\sim 60 \text{ K}$, it was necessary to “warm” the design to a nominal room temperature of $\sim 293 \text{ K}$ to provide manufacturers with fabrication parameters. In doing so, the

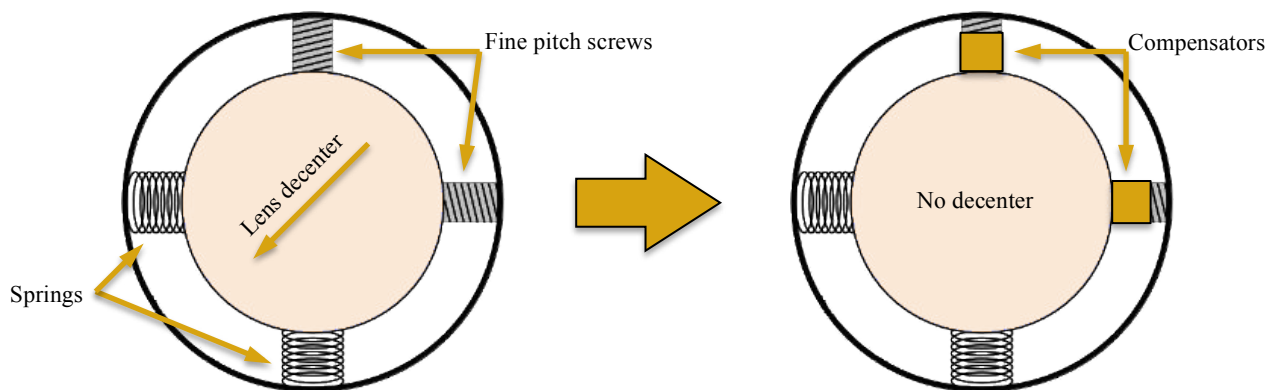


Figure 4. Drawing of the thermal decenter compensator design. The drawing on the left depicts the thermal decenter problem, in which the aluminum lens mount contracts more than the lens. This causes the lens center to move away from the optical axis. On the right is a depiction of a solution where high thermal contraction materials are placed between the screws and lenses. The lengths of these compensators are selected so that the thermal contraction of the screw + compensator + lens is equal to that of the mounting tube.

linear expansion of lenses as well as their changes in refractive indices were considered. Necessarily, thermal expansion of optomechanical elements was included.

Python scripts were written to aid in these efforts. They allow a user to supply a Zemax lens file and the code outputs a new file at the specified temperature. This method is favorable over Zemax's built-in temperature calculations since the scripts account for variable thermal contraction coefficients and rates of refractive index changes.

3.1 Thermal contraction

All thermal contraction and expansion is assumed to be linear. This approximation is expected to hold true for optomechanical elements, as they will all be made of the same aluminum alloy. Additionally, all of the crystals used as substrates for optical elements are of cubic structure, supporting the expectation that they will expand isotropically as the temperature is increased.

Lenses will be mounted within aluminum tubes where the center of each lens will be aligned with the optical axis using fine-pitch steel screws. Springs will apply force to keep the lens-edges in contact with the screw. In this setup, the aluminum tube will contract faster than the steel screw and glass/crystal lens. This will cause the center of the lens to move away from the optical axis, as shown on the left in Figure 4. To prevent this, high thermal contraction materials will be placed between the screws and lenses. These compensating materials will cause the average thermal contraction length of the lens, compensator and screw combination to be equal to that of the aluminum tube's radial contraction. This mounting-tube design is shown on the right of Figure 4.

3.2 Changing refractive indices

Refractive indices of lens substrates also vary with temperature. Finding materials with measured indices at cryogenic temperatures was a driving factor in the selection of substrates for RIMAS's optics. Fortunately a number of materials have been measured by the CHARMS project at GSFC and the results published^{8,9}.

4. SUMMARY

All of the design goals have been met for both the main optical system and the slit-imaging camera. The design includes photometric imaging capabilities as well as low and moderate resolution spectroscopy over a broad spectral range (0.9 – 2.4 μm). Additionally, the final system is small and light enough to be mounted on the DCT. The instrument's lenses have either been delivered or are expected in the near future. Discussions regarding diffractive elements are ongoing with manufacturers. The lens systems will be aligned in the laboratory at GSFC this fall. The previously described method for preventing aligned lenses from decentering as they are cooled will be tested. If successful, this design will be used in the final instrument. All optics are planned to be received, assembled and aligned by the end of 2013. In the spring of 2014, RIMAS will be commissioned on the DCT.

REFERENCES

- [1] Browder, S. J. and Ballard, S. S., "Low temperature thermal expansion measurements on optical materials," *Appl. Opt.*, 8(4), 793-798 (1969).
- [2] Butler, N., Klein, C. and others, "First Light with RATIR: An Automated 6-band Optical/NIR Imaging Camera," *Proc. SPIE* 8446, (2012).
- [3] Gehrels, N., Ramirez-Ruiz, E. and Fox, D. B., "Gamma-Ray Bursts in the Swift Era," *Annu. Rev. Astron. Astrophys.*, 47(1), 567-617 (2009).
- [4] Ikeda, Y., Kobayashi, N. and others, "Fabrication and current optical performance of a large diamond-machined ZnSe immersion grating," *Proc. SPIE* 7739, (2010).
- [5] Kuzmenko, P. J., Davis, P. J., Little, S. L. and Hale, L. C., "Materials and fabrication issues for large machined germanium immersion gratings," *Proc. SPIE* 6273, (2006).
- [6] Kuzmenko, P. J., personal communication, Jan. 24 (2013).
- [7] Levine, S. E., Bida, T. A. and others, "Status and performance of the Discovery Channel Telescope during commissioning," *Proc. SPIE* 8444, (2012).
- [8] Leviton, D. B., Frey, B. J. and Kvamme, T., "High accuracy, absolute, cryogenic refractive index measurements of infrared lens materials for JWST NIRCcam using CHARMS," *Proc. SPIE* 5904, (2005).
- [9] Leviton, D. B., Frey, B. J. and Madison, T. J., "Temperature-dependent refractive index of CaF₂ and Infrasil 301," *Proc. SPIE* 6692, (2007).
- [10] Nelson, J. D., Youngworth, R. N. and Aikens, D. M., "The cost of tolerancing," *Proc. SPIE* 7433, (2009).
- [11] Sebring, T. A., Dunham, E. W. and Millis, R. L., "The Discovery Channel Telescope: a wide-field telescope in Northern Arizona," *Proc. SPIE* 7433, (2004).
- [12] Trinh, C. Q., Ellis, S. C. and others, "GNOSIS: The First Instrument to Use Fiber Bragg Gratings for OH Suppression," *Astron. J.*, 145(2), article id. 51 (2013).
- [13] Veilleux, S., Bland-Hawthorn, J., Vogel, S. and Roy, R., "MOHSIS: The Maryland OH Suppression IFU System for the Discovery Channel Telescope," NSF Award Abstract #1207785, (2012).